Foam stability influenced by displaced fluids ~~in confined geometries~~and pore size of porous media

Mohammad Javad Shojaei[1], Kofi Osei-Bonsu[2], Simon Richman[1], Paul Grassia[3] and Nima Shokri*[1]

[1]School of Chemical Engineering and Analytical Science, University of Manchester, Manchester, UK

[2]Department of Petroleum Engineering, University of Wyoming, Laramie, WY The USA

[3]Department of Chemical and Process Engineering, University of Strathclyde, Glasgow G1 1XJ, United Kingdom

***Corresponding Author**

Dr. Nima Shokri

School of Chemical Engineering and Analytical Science

Room C26, The Mill

The University of Manchester

Sackville Street, Manchester, M13 9PL, UK

Tel: 0441613063980

Email: nima.shokri@manchester.ac.uk

19Group website: http://personalpages.manchester.ac.uk/staff/nima.shokri/

Abstract

Stability of foam in the presence of hydrocarbons is a crucial factor in the success of its use in various applications in porous media, such as soil remediation and enhanced oil recovery~~Stability of foam in the presence of hydrocarbons is a crucial factor in the success of foam in porous media applications such as soil remediation and enhanced oil recovery~~ (EOR). It is generally believed that shorter chain hydrocarbons with lower density and viscosity have more detrimental effect on foam stability than longer chain hydrocarbons. However, it is still unclear how ~~type of media and~~ pore size ~~distribution~~ of porous media could influence this behaviour. The main objective of the present study was to investigate the combined effect of the hydrocarbon chain length and hence the hydrocarbon's viscosity and pore size ~~distribution~~ of porous media on the foam stability~~–~~ and its displacement efficiency~~and propagation of flowing foam in porous media~~. ~~The correlation between foam stability in bulk systems and porous media was also investigated.~~ To this end, a systematic series of experiments was conducted using an empty Hele-Shaw cell and glass bead packs with different pore size ~~to investigate the effects of the oil viscosity, and pore size distribution on the stability of flowing foams~~. ~~The results from the bulk foam experiment showed that lower foam qualities increased foam stability in the presence of oil.~~ The results in Hele-Shaw cell and coarse and medium beads revealed that the lighter, less viscous oil (Isopar G)

was more destructive to foam. However, the results in the fine glass bead pack experiments, did not correlate well with this finding. In the fine bead pack, foam appeared to have higher displacement efficiency in the presence of the lighter, less viscous oil. Generally, our results suggest that the pore size of the porous medium plays a more important role on the foam displacement efficiency compare to the type of oil.~~The obtained results revealed foams had higher stability in coarse bead systems in the presence of lighter oil while its stability is greater in fine bead systems in the presence of heavier oil. The findings indicate that the combination of type of oil and properties of porous media influence stability of foam.~~

Keywords: Foam stability, Foam–oil interaction, Hele-Shaw cell, Pore size ~~distribution~~of porous media

1. INTRODUCTION

Foam is a dispersion of a large volume of gas in a small volume of liquid in which gas bubbles are made discontinuous by thin liquid films called lamellae.[1-3] Foam has a higher apparent viscosity compared to its constituents (gas and surfactant solution) making it a desirable mobility control agent for fluids displacements.[4-7] The stability of foam is one of the key determining parameters that influences the displacement efficiency of foam flooding projects.[8-11] Many studies have been conducted to investigate and describe the factors controlling foam stability. Derjaguin ~~et al.~~and Landau [12] introduced the theory of film disjoining pressure (Π), dependent upon film thickness (h), to explain the stability of a foam film. The disjoining pressure (Π) is defined as the sum of the repulsive positive electrostatic force per unit area (Π_{EL}) and attractive negative van der Waals force per unit area (Π_{VW}) according to classical DLVO theory.[13] At stable equilibrium the disjoining pressure of a lamellae film is equal to the capillary pressure, i.e., $\Pi = \Pi_{EL} + \Pi_{VW} = P_C$ which is the pressure difference across the interface of gas and surfactant (lamellae). Adsorption of surfactant to the gas liquid interface results in an increase of the repulsive positive electrostatic force (Π_{EL}) which stabilizes the lamellae. In contrast, attractive van der Waals forces destabilize the thin film. If $\Pi_{EL} > |\Pi_{VW}| + P_C$ foam will be stable, conversely, if the negative component is stronger ($\Pi_{EL} < |\Pi_{VW}| + Pc$), the foam will be destabilized.[14-15]

The effect of oil on foam stability has been explained by three mechanisms, i.e. entry of oil droplet into gas-liquid interface[16-17], spreading of oil on the gas-liquid interface[18], or formation of an unstable bridge across the lamella which destroys it.[19] So called, entry, spreading and bridging coefficients can be determined using interfacial tension and the signs of these coefficients are believed to govern stability. However, several studies showed that this theory may not be able to offer an accurate prediction of foam stability.[20-24] For example, Hadjiiski et al. [24] concluded that, no direct relation exists between the entering and spreading coefficients and the detrimental effect of oil on foam stability. Instead, they demonstrated that there is a strong correlation between the destabilising effects of oil and the magnitude of an “entry barrier” that is formed on the pseudoemulsion films between the oil droplet and the gas-liquid interface. The suppression of this oil drop entry is dictated by various surface forces (e.g. electrostatic, van der Waals) which are influenced by the physiochemical properties of the oil.

The effect of oil on foam stability within porous media is still not very well-understood as the presence of the medium adds another layer of complexity with only limited data available on foam-oil interactions in porous media. Indeed, although foam stability has been generally studied using bulk foam tests, several studies have demonstrated that bulk foam stability does not necessarily correlate with the stability of that same foam during flow in porous

media. DalIand et al. [25] reported there is no correlation between the stability of foam in bulk systems and porous media. Jones et al. [26] found apparent viscosity of foam in porous media is correlated to stability of foam in the bulk system in the absence of oil, but this correlation was not confirmed in the presence of oil. Osei-Bonsu et al. [27] showed stability of foam in bulk does not correlate with its effectiveness in oil displacement in porous media. Although~~,~~ the vast majority of research suggest that shorter chain hydrocarbons have more destabilising effect on foam than longer chain hydrocarbons with the shorter chain systems being typically less viscous [23, 28-31], it is still unclear how the combined effect of pore size ~~distribution~~ and hydrocarbon chain length and viscosity of the oil influence foam stability in porous media. The primary objective of this study was therefore to investigate the influence of the bead size (i.e. pore size) ~~distribution~~ on foam stability during oil displacement in porous media composed of packed bead. In addition, we investigate the influence of the viscosity of oil on foam stability during the displacement of oil by foam in a glass bead system and in a Hele-Shaw cell.

2. MATERIAL AND METHODS

2.1. Experimental Setup and Procedures

In order to investigate the effects of the various parameters on foam stability in bulk and porous media, two types of experiment were conducted. In both experiments a transparent cell (either empty or packed with glass beads) was initially saturated fully with oil/water. Pre-generated foam was then injected at a constant rate to displace the oil/water from the cell. The resulting displacement dynamics and foam-oil interactions were recorded using a camera. In the following more details about the experiments are described.

2.1.1. ~~Bulk Foam~~Hele-Shaw Cell Experiments

A customised Hele-Shaw cell (32 × 20 cm dimensions)~~, shown in Figure 6 in the APPENDIX,~~ was fabricated to investigate the dynamics of oil displacement by foam in bulk scale.

The Hele Shaw cell was similar to the one described in Osei-Bonsu et al.[32] It consisted of two transparent glass plates fixed to a Plexiglas frame. During the experiment these glass plates were clamped together, with a gasket sandwiched in between to create a small gap (1 mm) in which the two fluids (oil and foam) could flow. This gasket dictated the size of the gap (assuming the gasket was incompressible) and prevented any leakage of fluid around the edges of the cell. The top plate/frame contained a hole with a screw fitting at either end to allow

fluid to move in and out of the cell creating a flow path. A pressure transducer (Thurlby 30V-2A, with 0·3% accuracy and working range starting from 1 mbar) installed at the inlet of the Hele-Shaw cell. The outlet of the experiments was connected to the atmosphere.

Prior to each round of experiments, the surfactant solution was mixed again for 10 minutes using the magnetic stirring device, ensuring consistency between experiments. Before assembling the Hele-Shaw cell, each glass plate was cleaned thoroughly on both sides to remove any residual oil or deposits stuck to the surfaces. Initially the plates were washed using a combination of water and laboratory detergent. A cloth was then doused in Isopropanol and used to wipe the surfaces in order to dissolve and remove any residual oil, ensuring the results could not be influenced by these residues. It was vital that care was taken when handling and cleaning the glass plates to ensure the surfaces did not become scratched, maintaining a smooth and consistent flow path for oil and foam. This was also important for obtaining clearer images. The Hele-Shaw cell was then placed over a light box and the camera positioned above it using a clamp stand. The light box was used to ensure there was sufficient light to capture clear images showing a highly defined foam network, with individual lamellae easily distinguishable. The cell was then filled with oil using a syringe connected to a tube which was temporarily attached to the entrance of the cell. A metal tap was attached to the outlet to allow fluid to flow out of the cell and

into a collection beaker. During this oil injection the Hele-Shaw cell was tilted (at the outlet end) to ensure any gas bubbles trapped in the oil escaped at the exit. Once the oil reached the collection beaker (i.e. the cell was full) the outlet tap was closed. Two identical syringes (diameter of 19.3 mm) were filled with equal measures of surfactant solution (initially filled to 20 ml mark) and placed onto the syringe pump, where they were clamped in place. The corresponding syringe diameter was programmed into the pump and the rate was set according to the desired foam quality (see later calculations). A tube was attached to each syringe and then connected to the foam generator, with the tubes arranged either side of the gas inlet. The gas cylinder was connected to the foam generator via the mass flow controller. Initially, the gas cylinder outlet pressure was turned from 0 to 1 bar to introduce a gas supply. The FlowDDE program was opened on the lab computer and communication with the mass flow controller was initiated. FlowView was then used to control the gas flow rate. Both the gas and liquid flows were switched on simultaneously to begin generating foam. In this experiment the gas flow rate was kept constant at 2 ml/min. The flow rate of the surfactant solution was adjusted to 0.22 ml/min and 0.35 ml/min to produce the two different foam qualities chosen for this experiment – 90 % and 85 % respectively before the injection foam inside the system. Foam quality was calculated based on this equation $f_g = \frac{q_g}{q_{g+¿q_l}¿}$ that q_g and q_l are gas and surfactant

flow rates respectively. Each experiment was repeated at least three times to ensure the repeatability.

2.1.2. Experiments with Glass Beads

The cell packed with glass beads had a similar design to the Hele-Shaw cell described above. The gap size between the plates was 2 mm. This time, however, the two plates were fixed permanently in place using a number of screws fitted around the outside of the cell. This was necessary to allow glass beads to be packed into the cell sufficiently without damaging the glass plates. The inlet to this cell was very narrow to ensure that no glass beads could escape and potentially disrupt the packing. A fine metal mesh was fixed at the inlet of the model to prevent the glass beads from escaping and potentially disrupting the packing. Three different bead diameter ranges were used in this investigation: 0.50-1.00 mm and 1.25-1.55 mm and 0.15-0.21 mm. This enabled us to analyse the effects of grain/pore size of porous media on foam-oil interactions in porous media. The porosity of these three glass bead packings was approximately the same and equal to 35 %, but the permeability was different and equal to 24, 450 and 1100 D for fine, medium and coarse systems respectively. The glass bead was preferentially wet by surfactant. The cell contained a pressure transducer port located above the entrance of the cell to allow pressure drop to be measured. Like the Hele-Shaw cell, this bead pack

design allowed us to obtain a 2D visual description of foam-oil displacement dynamics.

At the beginning of each experiment the clean, empty cell had to be packed with glass beads. Initially, the cell was fixed vertically in place on the edge of the worktop using clamps, with the inlet in a downward-facing position. The inlet and pressure transducer port were temporarily blocked to prevent any fluid exiting the cell. The plate containing the outlet holes was removed to expose the outlet end of the cell. The cell was filled with oil (or water) and glass beads were then poured in, sinking to the bottom under gravity. The glass beads were inserted in stages, with compaction carried out using a metal ruler between each stage to ensure packing was as consistent as possible. Any excess oil that overflowed at the outlet was removed using a syringe. It was important that the same packing procedure (i.e. number of bead insertion/compaction stages) was used for each experiment to ensure that the porosities/total pore volumes were roughly the same (for experiments using the same bead size distribution). This ensured that packing inconsistencies did not distort any of the results and subsequent conclusions. Once the cell was packed, the detachable plate containing the outlet tubes was clamped to the outlet end of the cell. The glass bead pack was restored to its horizontal position and placed on top of the light box. The camera, which was connected to the lab computer, was then placed above the cell using a clamp stand. The precise positioning of the camera was

adjusted by looking at the live field of view displayed by its supporting software, Capture, on the lab computer. A pressure transducer was attached above the entrance of the cell. In this experiment the outlet was assumed to be at atmospheric pressure so the pressure drop was taken as the gauge pressure at the cell entrance. A collection beaker was placed beneath the outlet tubes to collect any fluid exiting the cell during the experiment. In this experiment the displacements of oils Isopar V and Isopar G were investigated in glass bead packs at three different bead sizes. Besides the detrimental effect of oil on foam stability, capillary suction influences the stability of foam in porous media [33]. Water displacement experiments with foam were performed at different pore size to see how capillary pressure influence foam stability. The experimental procedure of these experiments were exactly the same to oil displacement and just the type of fluid was changed.

In all the glass-bead experiments, the gas flow rate was the same as that used in the Hele-Shaw cell experiment (2 ml/min) and so the surfactant solution flow rate was set accordingly to achieve 85% foam quality before injection to the system. Each experiment was repeated at least three times to check the repeatability.~~However in this case the two plates were fixed permanently in place using a number of screws fitted around the outside of the cell. A fine metal mesh was fixed at the inlet of the model to prevent the glass beads from escaping and potentially disrupting the packing. A port for a pressure transducer~~

~~(Swagelok, UK) was created at the inlet of the cell to allow pressure measurements. The outlet consisted of three tubes attached to a detachable Plexiglas plate which was clamped to the end of the cell after bead packing. This plate was removed at the end of each experiment to allow the cell to be emptied of beads and thoroughly cleaned. Two different bead diameter ranges were used in this investigation: 0.50-1.00 mm and 1.25-1.55 mm. This enabled us to analyse the effects of grain/pore size distribution on foam-oil interactions in porous media. The porosity of these two glass bead packing was approximately the same and equal to 35 %. The glass bead was preferentially wet by surfactant.~~

2.1.3. Foam Generation and Fluid Properties

To generate foam, air and aqueous surfactant solution were pumped simultaneously, at specified and well-controlled flow rates, through a foam generator. Surfactant solution was injected by the syringe pump (Harvard Apparatus, USA with ±0.35% accuracy and working range from 0.0001 µl/hr to 100 ml/sec) while a mass flow controller (Bronkhorst, UK, with ±0,5% accuracy and working range from 1 ml/min to 100 ml/min) was used to deliver accurate and precise gas flow rates from the gas supply cylinder. [32]~~Surfactant~~

~~solution was injected by the syringe pump while a mass flow controller (Bronkhorst, UK) was used to deliver accurate and precise gas flow rates from the gas supply cylinder.~~

The same surfactant solution (the aqueous phase of the foam) was used in all experiments conducted in this investigation. This solution contained a 1:1 ratio of two different surfactants; Cocamidopropyl betaine (Cocobetaine) (The Soap Kitchen, UK, with 61789-40-0 CAS Number~~The Soap Kitchen, UK~~) and Sodium dodecyl sulphate (SDS) (Sigma, UK), each at 1% concentration (mass concentration) in a 0.1M NaCl aqueous solution. Osei-Bonsu et al.[23] showed that this surfactant provides more foam stability than the surfactants taken individually under our experimental conditions with the viscosity and interfacial tension being equal to 0.35~~interfacial tension equal 0.35~~ Pa.s and 0.13 mN/m respectively.[23] Two different oils, both belonging to the same hydrocarbon family (Isoparaffins), were used in these experiments to investigate the influence of oil properties on foam stability. It was important that these oils were of a similar type so that specific oil properties could be compared. The oils used were Isopar V and Isopar G (Sil-Mid Limited, UK); the former being the heavier and more viscous oil. Table 1 summarises the properties of these isoparaffin oils.

Table 1. Properties of the Isoparaffin Oils Used in ~~Our~~ these Experiments.

Isopar	Carbon chain	Dynamic viscosity 25°C (Pa.s)	Surface tension (mN/m) [23]
V	C14-C19	1.08	25.44
G	C10-C12	0.08	22.57

~~Isopar~~	~~Carbon chain~~	~~Density ($g\ cm^{-3}$)~~	~~Kinematic viscosity 25°C ($mm^2\ s^{-1}$)~~	~~Surface tension (mN/m)~~ [23]

2.2.

2.2.1. Image Processing

An automated monochromic camera (Dalsa Genie TS-2500) with a resolution of 2560 x 2048 pixels was used to capture high quality images of the foam evolution and oil displacement process over time. The captured images were processed and analysed using Image J software. The images were segmented and analysed one image sequence at a time (one experiment provided one image sequence). Initially, an image sequence was imported into ImageJ and the scale was set, converting the image pixel dimensions to a corresponding length in mm measured during the experiments. The horizontal dimension of 2560 pixels corresponded to a length of 228 mm. This enabled the software to calculate areas in mm^2 which therefore allowed us to calculate volumes of oil and gas (gap depth = 1 mm). The images were then segmented using the "Process>Find Edges" function which converted the images from greyscale to black and white.

This allowed the software to detect lines, curves and boundaries within the images which represented individual lamellae (foam films), oil/gas and oil/liquid interfaces and the perimeter around the cell (edge of the gasket). The contrast and brightness were adjusted using the “Adjust>Brightness/Contrast” function to allow these lines to become more distinguishable to ensure the software was able to detect them during the analysis.

The foam stability during oil displacement in the Hele-Shaw cell was quantified by calculating the volume of the released gas. It was expected that the higher the foam stability, the smaller volume of gas released from the foam network during the course of the displacement. Typical examples of the segmented images are presented in Figure 1~~Figure 1~~ showing the displacement of oil by foam in the Hele-Shaw cell (in the absence of glass beads). Figure 1~~Figure 1~~ qualitatively shows that as the foam progresses through the cell, the volume of the released gas from the foam increases as a result of the detrimental effect of oil on foam stability.

Once gas was released from the foam network, it either accumulated ahead of the foam front or along the walls of the Hele Shaw cell. This gas had a tendency to accumulate and form larger gas bubbles that were easily distinguishable from foam bubbles in terms of shape and size. Certain criteria were used to distinguish between foam bubbles and escaped gas as a result of destabilization. The first criterion was that the released gas bubble had to be located ahead of

the foam front or along the walls of the cell. The second criterion was that the gas bubble area had to be larger than 10 mm^2. This value was chosen after meticulously studying numerous images from a range of image sequences. It represented a bubble size larger than that of the usual generated foam bubbles with o.4 mm typical diameter.

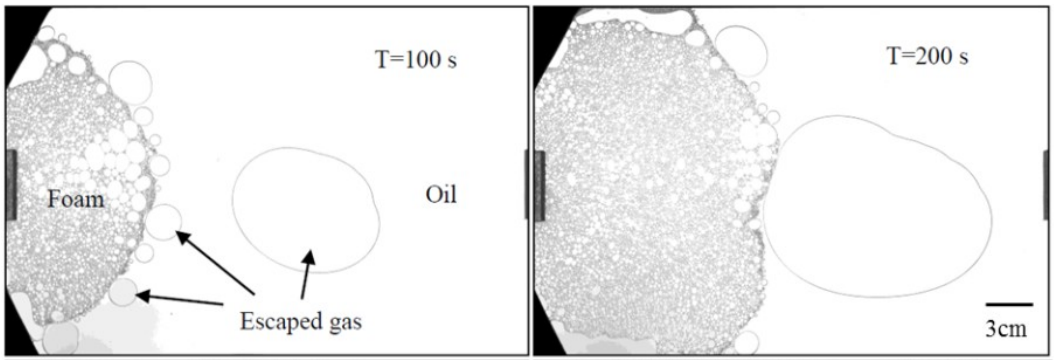

Figure 1.

~~Figure 1. A~~Two typical ~~sequence of~~ images taken at 100s time intervals showing the displacement of oil (Isopar G in this case) by foam in the Hele-Shaw cell at 85 % foam quality and 2 ml/min flow rate. The white colour in the image represents the gas and oil while the grey colour represents the lamellae.

3. RESULT AND DISCUSSION

3.1. Effect of Oil Type on Foam Stability in Hele Shaw Cell

Figure 2~~Figure 2~~ shows cumulative gas volume released (mm^3) from the foam network over time during oil displacement in the Hele-Shaw cell (in the absence

of glass beads) at two different foam qualities (85 and 90 %). The pressure drop of the system during the Hele-Shaw cell experiments was not so much (less than 10 mbar) that the compressibility effect of foam can be ignored.

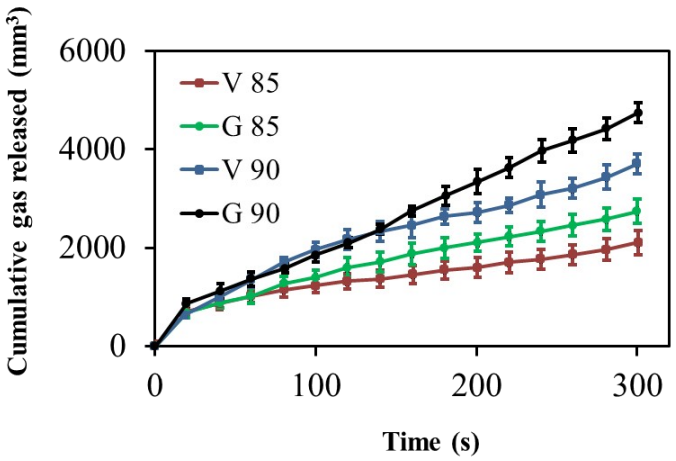

Figure 2.

~~Figure 2.~~ The cumulative volume of gas released from the foam network over time during oil displacement in the Hele-Shaw cell. V and G in the legend represent Isopar V and Isopar G respectively and the numbers represent the foam qualities in percentage. The error bars (half the length) indicate the standard deviation over 3 repeat measurements.

Figure 2~~Figure 2~~ demonstrates the influence of oil chain length (hence viscosity) and foam quality on the stability of foam in the presence of oil during Hele-Shaw cell experiments. It can be inferred from ~~the~~ Figure 2~~Figure 2~~ that more gas volume is released from foam during oil displacement at the higher foam quality (90%). This resulted in a final cumulative gas volume (at foam breakthrough point) that is approximately 66% higher for the higher foam

quality for the same oil; a substantial difference. The higher the volume of gas released the more the destabilisation of the foam by the oil. This implies that lamella rupture (i.e. coalescence) is much more prevalent at higher foam qualities.[32] The comparison between foam qualities in the presence of Isopar V (the more viscous oil) also follows the same trend as for the less viscous Isopar G and hence supports this interpretation. These results are in agreement with previous research on the influence of foam quality on foam stability in the presence of oil.[32, 34-36]

There are several reasons to explain why lower quality foams exhibit a higher tolerance to the defoaming activity of oil. One of the main reasons is that both foam films and the Plateau borders between those films are thicker, relative to bubble size. At lower foam qualities, these thicker films are more capable of suppressing the penetration of oil into ~~gas–~~gas-water interfaces, a mechanism which often leads to film rupture.[32] Thicker borders also ensure that there is a lower capillary suction pressure which means less liquid drainage within the films. Another possible reason for the increased stability at lower foam qualities is that the length of the foam films separating bubbles, in relation to total bubble perimeter, is lower meaning it is less probable that oil will enter the foam films in the first place and cause film rupture.

Figure 2~~Figure 2~~ indicates that the lighter oil shorter carbon chain Isopar G tends to have a more detrimental effect on foam stability. In fact, the rate of

foam coalescence (i.e. gas release) initially appeared to be very similar in the presence of both oils. However, as the experiments progressed and overall contact times between oil and foam increased, the rate of gas release from the foam in contact with Isopar G (lighter, less viscous) increased relative to Isopar V. A possible explanation for this is that as time progressed more of the lighter, less viscous oil was able to emulsify and form multiple smaller droplets ~~droplets~~ that could be drawn up into foam films and potentially destabilise them. This can be attributed to the fact that less viscous oils emulsify more quickly which would consequently accelerate the rate of ~~lamellae~~ lamellas collapse in relation to the more viscous oil.[37]

The final cumulative volume of gas released in both experiments (85% and 90% quality) was approximately 30% higher in the presence of Isopar G than Isopar V. Comparing this to the effect of foam quality discussed in the previous section, a 5% increase in foam quality appeared to have a much stronger influence on foam stability in the presence of oil than the differences between the two oils themselves (66% difference compared with 30%).

3.1.1. ~~Oil Displacement Efficiency~~

~~Figure 3 shows the oil recovery factor (defined as the volume of oil recovered from the cell divided by the initial volume of oil in the cell) versus time at two foam qualities in the Hele-Shaw cell.~~

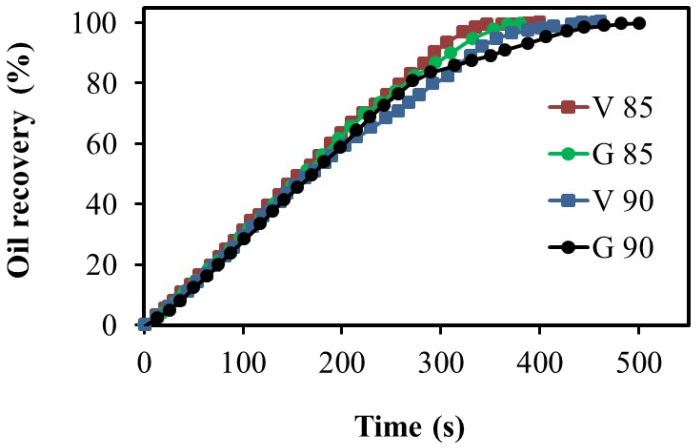

Figure 3. The oil recovery factor vs time during oil displacement in the Hele-Shaw cell for each oil-foam combination. V and G in the legend represent Isopar V and Isopar G respectively. The numbers represent the foam qualities.

Figure 3 shows there are no substantial differences between the displacements of the different oils over time in our experiments with the Hele-Shaw cell (in the absence of glass beads). The gas that was released from the foam remained accumulated behind the oil (at the foam front) until the later stages of the displacement process which meant the total volume of displacing fluid within the cell was roughly the same throughout. It does appear, however, that overall more time was required to reach 100% recovery during the displacement of Isopar G. This can be attributed to the high level of foam destruction in the presence of this oil meaning the foam was less effective in displacing the oil. The reason for this is that when the large pockets of gas (resulting from foam collapse) ahead of the foam front reached the exit of the cell they had a tendency to escape through the the exit of the model more quickly than the oil

~~due to differences in density[37]. Since these escaping gas volumes were generally larger in the presence of Isopar G, a larger volume of displacing fluid was lost as these large gas pockets broke away from the foam front. This effectively slowed the rate of oil recovery, particularly during later stages of the displacement process as shown by the diminishing slope of the line representing Isopar G in Figure 3.~~

3.2. Effect of Type of Oil on Foam Stability in ~~Coarse and Fine Glass Bead Packings~~Porous Media with Different Pore Size

~~Figure 4 illustrates the displacement of oil/water by foam after 1.9 PV foam injection in each experiment in coarse and fine-textured glass beads packs.~~

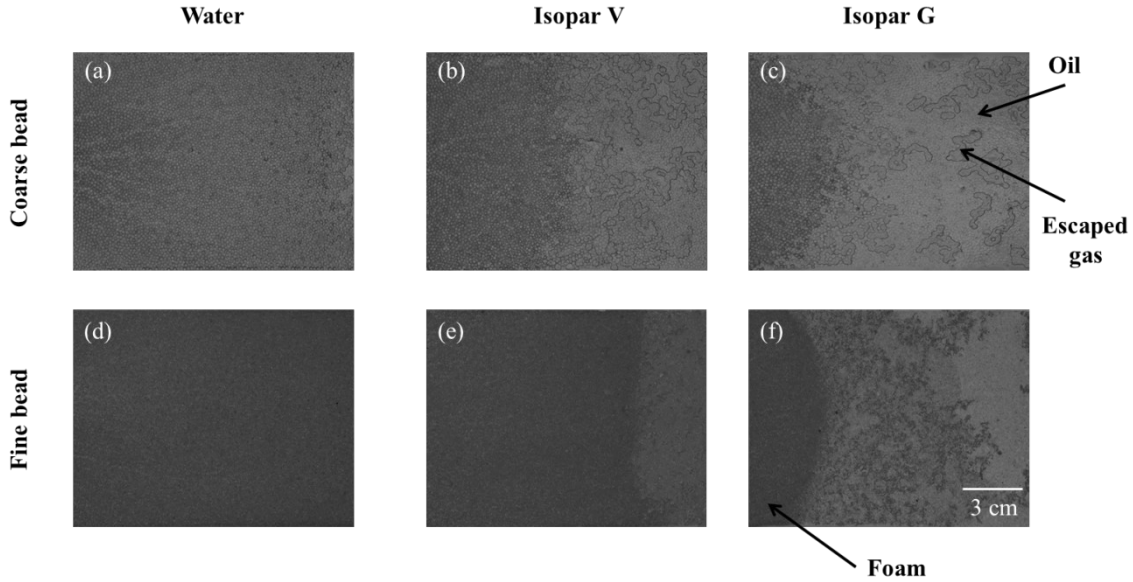

~~**Figure 4.** Images (a-f) show the displacement of oil/water by foam after 1.9 PV foam injection in each experiment. Images (a-c) represent the packs with the~~

~~larger grain sizes (1.25-1.55 mm) and images (d-f) represent the pack with the smaller grain sizes (0.5-1 mm).~~

~~Figure 4 demonstrates the destructive effect of oil on foam in porous media by comparing oil displacement with water displacement. Images (a) and (d) indicate very little foam destruction in the presence of water with no gas breakthrough. Conversely, the rest of the images in Figure 4 reveal large areas of gas fingers through the oil phase which signify substantial levels of foam destruction. Figure 4 also show that after 1.9 PV foam injection the foam front had propagated much further during the displacement of water implying that the foam was much more stable in the presence of water than oil.~~

In contrast to the Hele-Shaw cell, it was challenging to measure the amount of gas released from the foam in the experiments with porous media. It is hypothesised that ~~T~~the gas released as a result of foam destruction was able to penetrate the glass bead-pack rapidly, forming gas channels connected to the outlet rather than accumulating ahead of the foam front in gas pockets. Accordingly, area within the model occupied by foam (foam saturation) and the pressure drop across the glass bead pack were measured as an indication of foam stability and its efficiency for fluid displacement. ~~Foam with higher stability could propagate more effectively through the model with more piston-like pattern that provides more pressure drop across the medium.~~

~~Figure 5~~Figure 3 shows foam saturation, defined as the ~~area~~ volume occupied by foam relative to total ~~cell~~ pore ~~area~~volume, and the pressure drop during the displacement of oil/water by foam in the ~~coarse and fine bead pack~~porous media with different pore size.

444

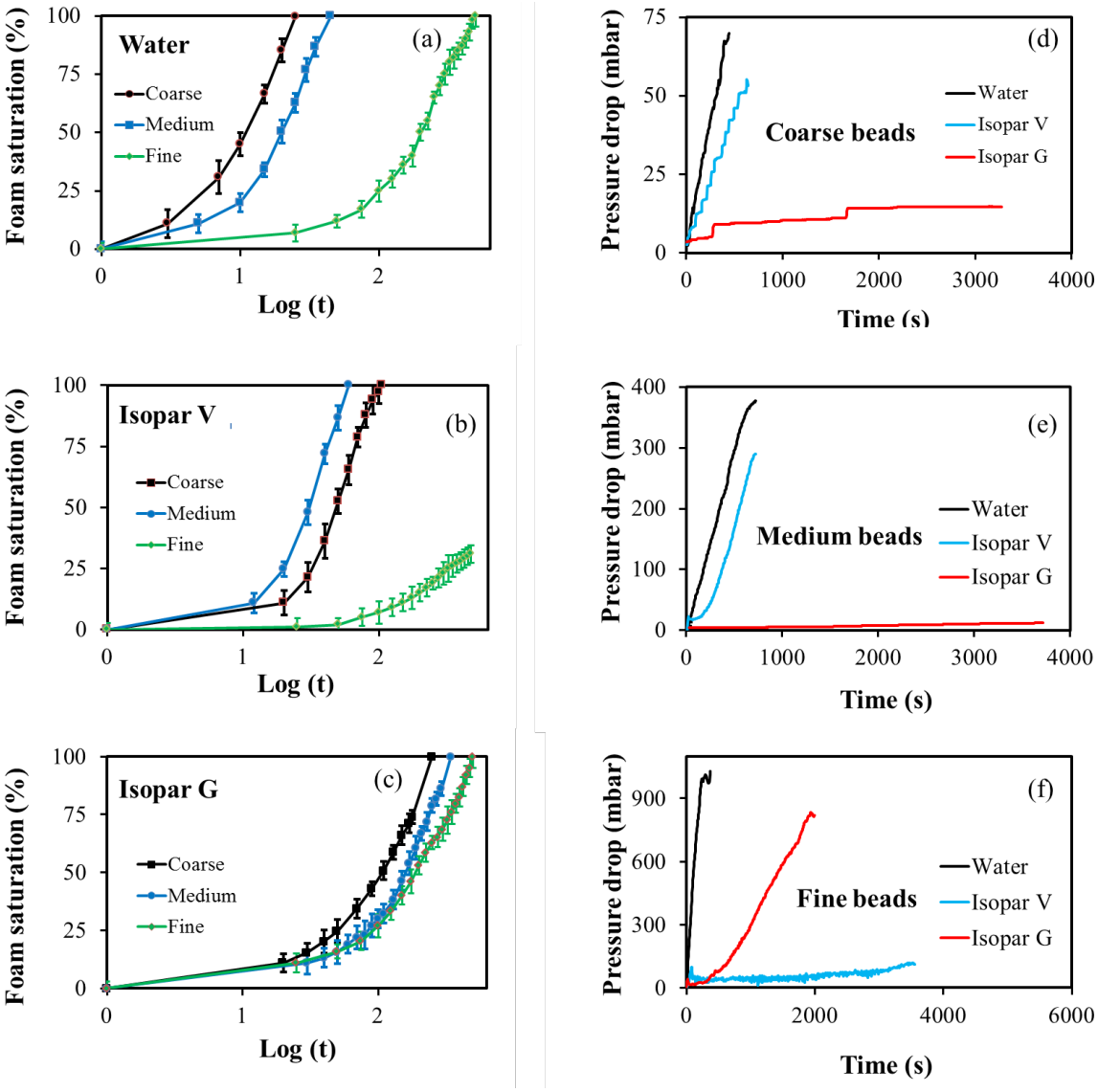
Water
(a)
Coarse
Medium
Fine
Foam saturation (%)
Log (t)
Isopar V
(b)
Isopar G
(c)
Coarse beads
(d)
Water
Isopar V
Isopar G
Pressure drop (mbar)
Time (s)
Medium beads
(e)
Fine beads
(f)

445

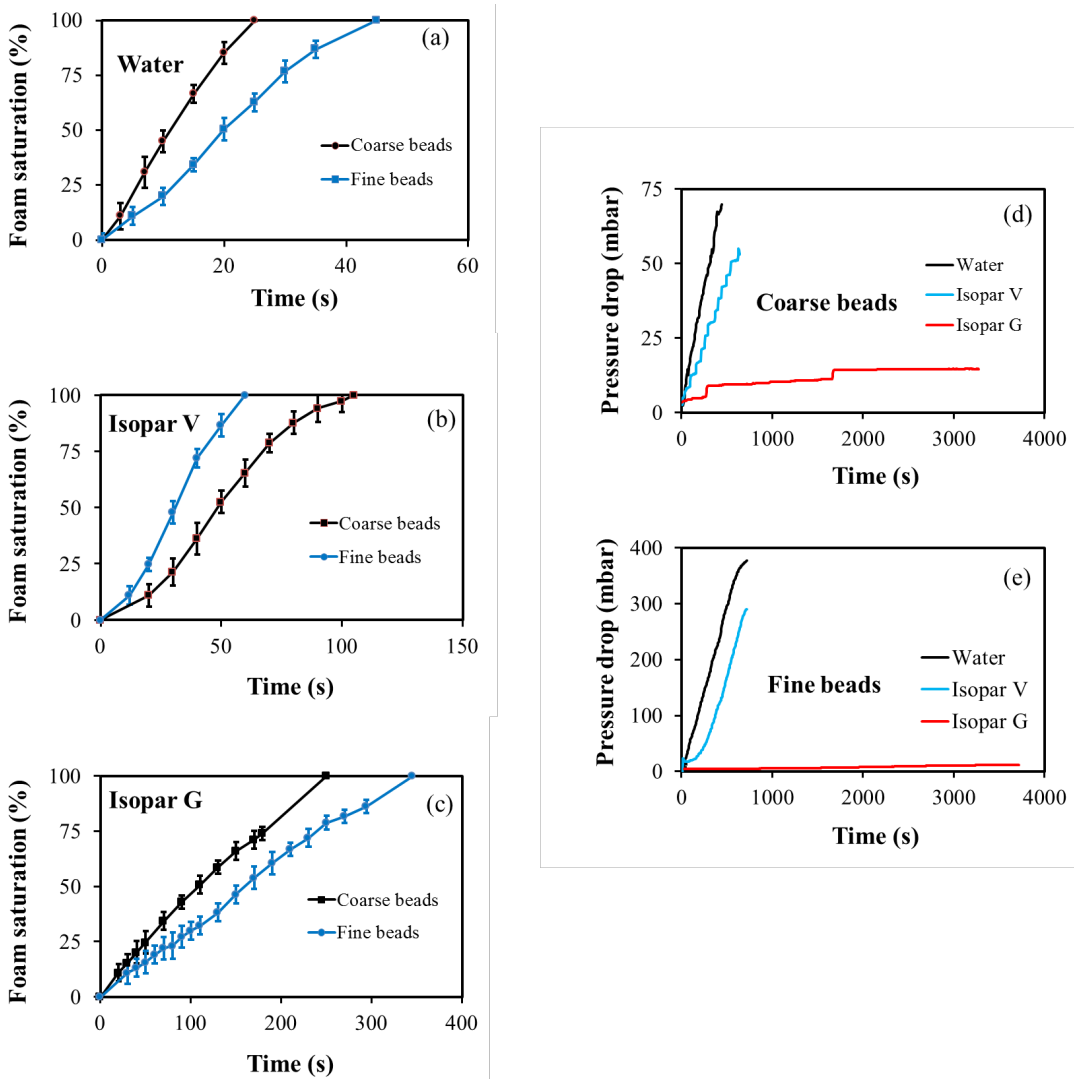

446

447Figure 3.

~~Figure 5.~~ (a), (b)~~, and~~ (c) ~~–~~Foam saturation as a function of logarithm time (second) ~~in coarse and fine beads packs displacing water, Isopar V and Isopar G, respectively.~~ during the displacement of water, Isopar V and Isopar G respectively (d), (e) and (~~e~~f) Pressure drop vs time during the displacement of oil/water by foam ~~in the coarse and fine bead packs, respectively~~ at coarse, medium and fine sand pack beads respectively. The gas flow rate and foam quality were 2 ml/min and 85 % respectively. The error bars (half the length) ~~The error bars~~ indicate the standard deviation over 3 repeat measurements.

~~Figure 5~~ Figure 3 clearly demonstrates the destructive effect of oil on foam stability and its displacement efficiency in porous media. Saturation of foam and the pressure of the system are higher in the presence of water compared to oil when the other experimental conditions are the same. Moreover, Figure 3 (a) in the presence of water appear to show a more significant difference between the behaviour of foam as more time is needed to ensure that the foam saturates all the system as the pore size of the porous media decreases. This suggests that a significantly larger amount of foam was destroyed during water displacement in the finer glass bead pack due to capillary suction. ~~. This suggests higher coalescence rate in the fine glass bead pack due to capillary suction.~~ In porous media, capillary pressure ~~drop~~ can be considered as the force per area required for squeezing a hydrocarbon droplet through a pore throat, working against the

interfacial tension between oil and water. This capillary pressure is higher ~~for~~in smaller pore ~~diameters~~. Hence this increased capillary pressure ~~may~~ have destabilised the foam to a greater extent, making foams films more susceptible to rupture as they attempt to force oil through tighter pore constrictions.[33]

Figure 3 shows foam provided higher pressure drop as the pore size of the sand pack decreases. This is due to the lower permeability of finer sand pack. As the foam is in general a compressible fluid, it seems compressibility could influence the texture of the foam and its saturation. The texture of foam is generally determined by the porous medium in which it resides and its pressure, in other words bubble sizes tend to be dictated by pore sizes as the pressure increases. It follows that pre-generated foam (used in this investigation) is re-shaped and re-textured by the porous medium through which it is injected [38]~~{Kovscek, 1993 #2477}~~. Accordingly, we can expect foam would have higher foam quality in the upstream of the system compare to downstream as the outlet of the system is connected to atmosphere and the inlet of the system is influenced by the pressure inside the porous media. Lower foam quality in the upstream has more liquid saturation that made it more tolerant to detrimental effect of oil and capillary suction. This help the system to increase its foam saturation as the time passed.

Comparing Figure 3 (b) with (c) shows similar to Hele-Shaw cell, heavier oil (Isopar V) provide more foam stability in the medium and coarse bead system.

~~(a) foam has higher saturation in coarse bead compare to fine bead in water displacement with water. This suggests higher coalescence rate in the fine glass bead pack due to capillary suction. In porous media, capillary pressure drop can be considered as the force per area required squeezing a hydrocarbon droplet through a pore throat, working against the interfacial tension between oil and water. This capillary pressure is higher for smaller pore diameters. Hence this increased capillary pressure may have destabilised the foam to a greater extent, making foams films more susceptible to rupture as they attempt to force oil through tighter pore constrictions.[37]~~

~~If we relate foam saturation to foam stability~~ However, ~~Figure 5~~Figure 3 (b) shows the stability of foam in the presence of Isopar V is greater in the ~~fine~~ medium bead system compare to coarse bead system ~~and in the fine bead system compare to the coarse bead system~~ and for Isopar G stability is greater in coarse bead systems compare to ~~fine~~ medium bead ones as Figure 3 (c) shows. Visual observations of displacement of oil by foam showed two fronts. The first front (further back) was the front of foam and second front (further forward) was the front of the escaped gas that resulted from foam coalescence. The second front was not effective to displace all the oil and there were some unswept oil areas. Visual inspections showed this unswept oil did not have a high detrimental effect on the foam for heavier oil in ~~fine~~ medium bead systems and the first front propagated effectively and achieved higher foam saturation.

However, these unswept areas had a detrimental effect on foam for lighter oil (Isopar G) and delayed the formation of a strong foam bank in ~~fine~~ medium bead systems. ~~Figure 5 (c) suggests Isopar G permits higher foam stability in coarse bead systems compared to fine bead ones. It can be explained by higher rate of foam coalescence in fine bead system by capillary suction pressure as discussed before.~~

~~Figure 5 (d) and (e) show the pressure drop in oil displacement is lower than in the water displacement experiment. This could be explained by residual, unswept oil within the glass bead pack destroying some of the foam giving it a coarser texture. This foam destruction would reduce the apparent viscosity of the foam, due to a decrease in the number of foam lamellae, which would be characterised by a lower pressure drop.~~[33] Figure 3 shows foam behaves significantly different in fine bead pack as the type of oil changes. This difference is also reciprocated in the pressure drop curves in Figure 3 (f). This implies that the foam was more effective to displace fluid in the presence of the lighter, less viscous Isopar G, which contradicts our original finding made during the foam displacement in coarse and medium beads and Hele-Shaw cell. It was observed that the released gas resulted from detrimental effect of oil and capillary suction fingered more in the low permeability medium. Accordingly, the subsequent injection of foam followed these preferential flow paths and

produced from the outlet without propagation to the other parts of the system. As Figure 3 (b) shows foam in the fine glass bead packs was not able to propagate across the whole of the cell during heavier oil displacement (Isopar V) due to the high viscous fingerings.

~~Moreover, Figure 5 shows foam provided higher pressure drop (higher apparent viscosity) in fine bead pack than the coarse one. This is due to fine bead packing having lower permeability and hence producing higher pressure drop for fluid displacement. These results suggest both the type of oil and the pore size distribution of porous media control stability of foam.~~

SUMMARY AND CONCLUSION

Oil displacement experiments were carried out in a Hele-Shaw cell and glass bead packs to investigate the combined effect of type of oil and pore size ~~distribution~~ of porous media on foam stability and its displacement efficiency. ~~The influence of oil on foam stability inside and outside (bulk foam) of porous media was studied as well.~~ The effects of foam quality studied in the Hele-Shaw cell ~~(bulk foam)~~ showed conclusively that lower foam qualities result in formation of foam with an increased tolerance to the destructive effects of oil.

The type of oil appeared to have a strong influence on foam stability during oil displacement in the Hele-Shaw cell and porous media. Foam showed lower foam stability and displacement efficiency in the presence of ~~A much more~~

~~substantial release of gas from the foam was observed during the displacement~~ ~~of~~ the lighter, less viscous oil (Isopar G) ~~which was indicative of greater foam destabilisation in the presence of this oil~~in Hele-Shaw cell and coarse and medium porous media.

The effect of oil type in the fine glass bead experiment did not appear to correlate well with the pronounced effects displayed in the Hele-Shaw cell and coarser porous media. The fine bead pack actually demonstrated the opposite effect as the foam appeared to have higher displacement efficiency in the presence of lighter oil. Overall these results suggest that the geometry of the porous medium (i.e. average pore size) has a much more important influence on the foam displacement efficiency in the presence of oil than the type of oil itself.~~Taken together, these results suggest that the combined effect of type of oil and property of porous media determine the foam stability.~~

ACKNOWLEDGMENTS

We would like to acknowledge the UK Engineering and Physical Sciences Research Council (EPSRC) for providing the PhD studentship for ~~Muhammad~~ Mohammad Javad Shojaei.

AUTHOR INFORMATION

Corresponding Author

E-mail: nima.shokri@manchester.ac.uk.

Notes

The authors declare no competing financial interest.

APPENDIX

Figure 6 shows the experimental set-up used in the Hele-Shaw cell experiments.

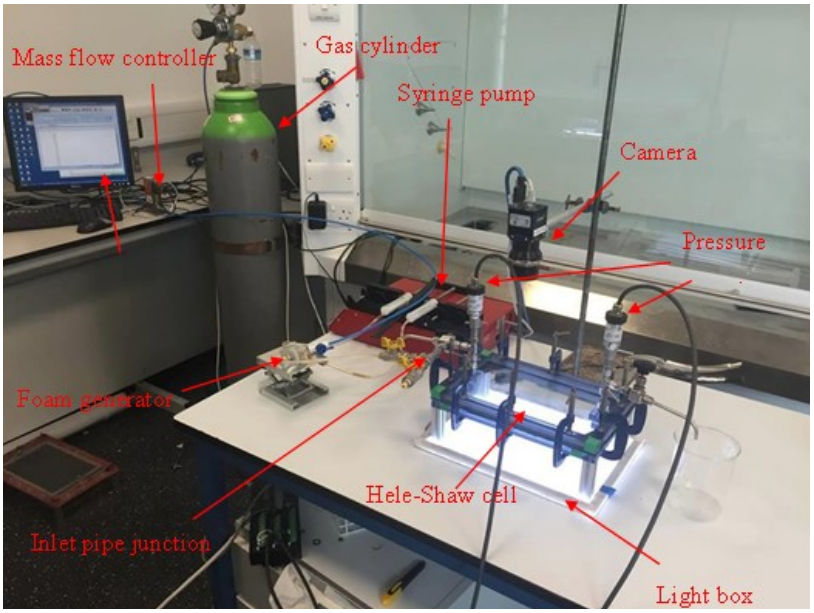

Figure 6. Experimental setup used to investigate oil displacement by foam in a Hele-Shaw cell. Individual equipment is labelled in red.

REFERENCES

1. Solbakken, J. S.; Skauge, A.; Aarra, M. G., Foam performance in low permeability laminated sandstones. *Energy & Fuels* 2014, *28* (2), 803-815.
2. Hosseini-Nasab, S. M.; Zitha, P. L., Investigation of chemical-foam design as a novel approach toward immiscible foam flooding for enhanced oil recovery. *Energy & Fuels* 2017, *31* (10), 10525-10534.
3. Li, S.; Li, Z.; Lu, T.; Li, B., Experimental study on foamy oil flow in porous media with Orinoco Belt heavy oil. *Energy & Fuels* 2012, *26* (10), 6332-6342.
4. Eftekhari, A. A.; Farajzadeh, R., Effect of foam on liquid phase mobility in porous media. *Scientific Reports* 2017, *7*.
5. Li, Z.; Rossen, W. R.; Nguyen, Q. P., Three-dimensional modeling of tracer experiments to determine gas trapping in foam in porous media. *Energy & Fuels* 2010, *24* (5), 3239-3250.
6. Tao, J.; Dai, C.; Kang, W.; Zhao, G.; Liu, Y.; Fang, J.; Gao, M.; You, Q., Experimental Study on Low Interfacial Tension Foam for Enhanced Oil Recovery in High-Temperature and High-Salinity Reservoirs. *Energy & Fuels* 2017, *31* (12), 13416-13426.
7. Bagheri, S. R., Experimental and Simulation Study of the Steam–Foam Process. Part 2: The Effect of Oil on Foam Generation. *Energy & Fuels* 2017, *31* (3), 2687-2696.
8. Zhu, T.; Ogbe, D.; Khataniar, S., Improving the foam performance for mobility control and improved sweep efficiency in gas flooding. *Industrial & engineering chemistry research* 2004, *43* (15), 4413-4421.
9. AlYousef, Z.; Almobarky, M.; Schechter, D., Enhancing the Stability of Foam by the Use of Nanoparticles. *Energy & Fuels* 2017, *31* (10), 10620-10627.
10. Hurtado, Y.; Beltran, C.; Zabala, R. D.; Lopera, S. H.; Franco, C. A.; Nassar, N. N.; Cortés, F. B., Effects of Surface Acidity and Polarity of SiO2 Nanoparticles on the Foam Stabilization Applied to Natural Gas Flooding in Tight Gas-Condensate Reservoirs. *Energy & Fuels* 2018, *32* (5), 5824-5833.
11. Nguyen, P.; Fadaei, H.; Sinton, D., Pore-scale assessment of nanoparticle-stabilized CO2 foam for enhanced oil recovery. *Energy & Fuels* 2014, *28* (10), 6221-6227.
12. Derjaguin, B.; Landau, L., The theory of stability of highly charged lyophobic sols and coalescence of highly charged particles in electrolyte solutions. *Acta Physicochim. URSS* 1941, *14* (633-52), 58.
13. Kovscek, A.; Radke, C., Fundamentals of foam transport in porous media. ACS Publications: 1994.
14. Farajzadeh, R.; Andrianov, A.; Krastev, R.; Hirasaki, G.; Rossen, W. R., Foam–oil interaction in porous media: implications for foam assisted enhanced oil recovery. *Advances in colloid and interface science* 2012, *183*, 1-13.
15. Exerowa, D.; Kruglyakov, P. M., *Foam and foam films: theory, experiment, application*. Elsevier: 1997; Vol. 5.
16. Harkins, W. D., A general thermodynamic theory of the spreading of liquids to form duplex films and of liquids or solids to form monolayers. *The Journal of Chemical Physics* 1941, *9* (7), 552-568.
17. Robinson, J.; Woods, W., A method of selecting foam inhibitors. *Journal of Chemical Technology and Biotechnology* 1948, *67* (9), 361-365.
18. Lau, H.; O'Brien, S., Effects of spreading and nonspreading oils on foam propagation through porous media. *SPE reservoir engineering* 1988, *3* (03), 893-896.
19. Garrett, P. R., *The science of defoaming: theory, experiment and applications*. CRC Press: 2016; Vol. 155.
20. Basheva, E. S.; Ganchev, D.; Denkov, N. D.; Kasuga, K.; Satoh, N.; Tsujii, K., Role of betaine as foam booster in the presence of silicone oil drops. *Langmuir* 2000, *16* (3), 1000-1013.
21. Vikingstad, A. K.; Skauge, A.; Høiland, H.; Aarra, M., Foam–oil interactions analyzed by static foam tests. *Colloids and Surfaces A: Physicochemical and Engineering Aspects* 2005, *260* (1), 189-198.

22. Koczo, K.; Lobo, L.; Wasan, D., Effect of oil on foam stability: aqueous foams stabilized by emulsions. *Journal of colloid and interface science* 1992, *150* (2), 492-506.
23. Osei-Bonsu, K.; Shokri, N.; Grassia, P., Foam stability in the presence and absence of hydrocarbons: from bubble-to bulk-scale. *Colloids and Surfaces A: Physicochemical and Engineering Aspects* 2015, *481*, 514-526.
24. Hadjiiski, A.; Denkov, N. D.; Tcholakova, S.; Ivanov, I. B., *Role of entry barriers in the foam destruction by oil drops*. Marcel Dekker: New York: 2002.
25. Dalland, M.; Hanssen, J. E.; Kristiansen, T. S., Oil interaction with foams under static and flowing conditions in porous media. *Colloids and Surfaces A: Physicochemical and Engineering Aspects* 1994, *82* (2), 129-140.
26. Jones, S.; Van Der Bent, V.; Farajzadeh, R.; Rossen, W.; Vincent-Bonnieu, S., Surfactant screening for foam EOR: Correlation between bulk and core-flood experiments. *Colloids and Surfaces A: Physicochemical and Engineering Aspects* 2016, *500*, 166-176.
27. Osei-Bonsu, K.; Grassia, P.; Shokri, N., Relationship between bulk foam stability, surfactant formulation and oil displacement efficiency in porous media. *Fuel* 2017, *203*, 403-410.
28. Vikingstad, A. K.; Skauge, A.; Høiland, H.; Aarra, M., Foam–oil interactions analyzed by static foam tests. *Colloids and Surfaces A: Physicochemical and Engineering Aspects* 2005, *260* (1-3), 189-198.
29. Lee, J.; Nikolov, A.; Wasan, D., Stability of aqueous foams in the presence of oil: on the importance of dispersed vs solubilized oil. *Industrial & Engineering Chemistry Research* 2012, *52* (1), 66-72.
30. Simjoo, M.; Rezaei, T.; Andrianov, A.; Zitha, P., Foam stability in the presence of oil: effect of surfactant concentration and oil type. *Colloids and Surfaces A: Physicochemical and Engineering Aspects* 2013, *438*, 148-158.
31. Schramm, L. L.; Novosad, J. J., The destabilization of foams for improved oil recovery by crude oils: effect of the nature of the oil. *Journal of Petroleum Science and Engineering* 1992, *7* (1-2), 77-90.
32. Osei-Bonsu, K.; Shokri, N.; Grassia, P., Fundamental investigation of foam flow in a liquid-filled Hele-Shaw cell. *Journal of colloid and interface science* 2016, *462*, 288-296.
33. Khatib, Z.; Hirasaki, G.; Falls, A., Effects of capillary pressure on coalescence and phase mobilities in foams flowing through porous media. *SPE reservoir engineering* 1988, *3* (03), 919-926.
34. Svorstol, I.; Vassenden, F.; Mannhardt, K. In *Laboratory studies for design of a foam pilot in the Snorre field*, SPE/DOE improved oil recovery symposium, Society of Petroleum Engineers: 1996.
35. Minssieux, L., Oil displacement by foams in relation to their physical properties in porous media. *Journal of Petroleum Technology* 1974, *26* (01), 100-108.
36. Sydansk, R. D., Foam for improving sweep efficiency in subterranean oil-bearing formations. Google Patents: 1992.
37. Talebian, S. H.; Masoudi, R.; Tan, I. M.; Zitha, P. L. In *Foam assisted CO2-EOR; concepts, challenges and applications*, SPE Enhanced Oil Recovery Conference, Society of Petroleum Engineers: 2013.
38. Kovscek, A.; Radke, C. *Fundamentals of foam transport in porous media*; Lawrence Berkeley Lab., CA (United States): 1993.